

# A Framework for Control Channels Applied to Reconfigurable Intelligent Surfaces

Fabio Saggese, *Member, IEEE*, Victor Croisfelt, *Student Member, IEEE*,  
 Radosław Kotaba, Kyriakos Stylianopoulos, *Student Member, IEEE*, George C.  
 Alexandropoulos, *Senior Member, IEEE*, and Petar Popovski, *Fellow, IEEE*

## Abstract

The research on Reconfigurable Intelligent Surfaces (RISs) has dominantly been focused on physical-layer aspects and analyses of the achievable adaptation of the propagation environment. Compared to that, the questions related to link/MAC protocol and system-level integration of RISs have received much less attention. This paper addresses the problem of designing and analyzing control/signaling procedures, which are necessary for the integration of RISs as a new type of network element within the overall wireless infrastructure. We build a general model for designing control channels along two dimensions: *i*) allocated bandwidth (in-band and out-of band) and *ii*) rate selection (multiplexing or diversity). Specifically, the second dimension results in two transmission schemes, one based on channel estimation and the subsequent adapted RIS configuration, while the other is based on sweeping through predefined RIS phase profiles. The paper analyzes the performance of the control channel in multiple communication setups, obtained as combinations of the aforementioned dimensions. While necessarily simplified, our analysis reveals the basic trade-offs in designing control channels and the associated communication algorithms. Perhaps the main value of this work is to serve as a framework for subsequent design and analysis of various system-level aspects related to the RIS technology.

## Index Terms

Reconfigurable intelligent surfaces, control channel, protocol design, performance analysis.

This work was partly supported by the Villum Investigator grant “WATER” from the Villum Foundation, Denmark, and by the EU H2020 RISE-6G project under grant number 101017011. F. Saggese, V. Croisfelt, R. Kotaba, and P. Popovski are with the Connectivity Section of the Department of Electronic Systems, Aalborg University, Aalborg, Denmark (e-mails: {fasa, vcr, rak, petarp}@es.aau.dk). K. Stylianopoulos and G. C. Alexandropoulos are with the Department of Informatics and Telecommunications, National and Kapodistrian University of Athens, Panepistimiopolis Ilissia, 15784 Athens, Greece (e-mails: {kstylianop, alexandg}@di.uoa.gr).

## I. INTRODUCTION

Reconfigurable Intelligent Surfaces (RISs) constitute a promising technology that in recent years has received significant attention within the wireless communication research community [1]. The main underlying idea is to electronically tune the reflective properties of an RIS in order to manipulate the phase, amplitude, and polarization of the incident electromagnetic waves [2]. This results in the effect of creating a propagation environment that is, at least partially, controlled [3]. RISs can be fabricated with classical antenna elements controlled through switching elements or, more advanced, can be based on metamaterials with tunable electromagnetic properties [4]. In the context of 6G wireless systems, the RIS technology has been identified as one of the cost-effective solutions to address the increasing demand for higher data rates, reduced latency, and better coverage. In particular, an RIS can improve the received signal strength and reduce interference by directing signals to intended receivers and away from non-intended ones; this leads to applications aiming increased communication security [5] and/or reduced electromagnetic field exposure [6]. RISs can also extend the coverage of wireless communication systems by redirecting the signals to areas that are difficult to reach using conventional means.

In terms of challenges related to the RIS technology, the dominant part of the literature concerning RIS-aided communication systems deals with physical-layer (PHY) aspects. Recent studies have explored physics-based derivation of channel models, extending plane wave expansions beyond the far-field approximation [7]. While many papers have investigated the potential benefits of RIS-assisted systems in terms of spectral and energy efficiency (see, *e.g.*, [8]), others have concentrated on optimizing the RIS configuration alone or jointly with the beamforming at the base station (BS). On the other hand, several works have focused on designing and evaluating channel estimation (CE) methods in the presence of RISs, either relying on the cascaded end-to-end channel when dealing with reflective RISs [9], or focusing on the individual links using simultaneous reflecting and sensing RISs [10]. The latter design belongs to the attempts to minimize the RIS reconfiguration overhead, which can be considerably large due to the expected high numbers of RIS elements [11] or hardware-induced non linearities [8]. A different research direction bypasses explicit channel estimation and relies on beam sweeping methods [12]. Accordingly, within each coherent channel block, the RIS is scheduled to progressively realize phase configurations from a predefined codebook, for the end-to-end system to discover the most suitable reflective beamforming pattern [13]–[16]. The beams are practically optimized for

different purposes [17], possibly comprising hierarchical structures [15], [18].

Within the existing research literature, the questions related to link/MAC protocol and system-level integration of RISs have received much less attention as compared to PHY topics. Specifically, the aspects related to control/signaling procedures have been largely neglected, despite the fact that those procedures are central to the integration of RISs as a new type of network element within existing wireless infrastructure. In this regard, it is important to study the RIS control from two angles. *First*, as an enabler of the new features that come with the RIS technology and a component that ensures its proper operation in general. Assessing this aspect requires looking into the required performance of the control channel in terms of, for example, rate, latency, and, not the least, reliability. *Second*, control procedures introduce an overhead in the system, such that it is important to characterize the trade-off between spending more time and resources on the auxiliary procedures (such as more robust channel estimation or optimization of the RIS reflection pattern) versus data transmission. This paper aims to fill this important knowledge gap, relevant to both theory and practice of RIS-aided communications, by providing a systematic analysis of the control architecture options and the associated protocols.

#### A. Related literature

One of the first works focusing on fast RIS programmability [13] presented a multi-stage configuration sweeping protocol. By tasking the RIS to dynamically illuminate the area where a user equipment (UE) is located, a downlink transmission protocol, including sub-blocks of UE localization, RIS configuration, and pilot-assisted end-to-end channel estimation, was introduced in [14]. In [15], a fast near-field alignment scheme for the RIS phase shifts and the transceiver beamformers, relying on a variable-width hierarchical RIS phase configuration codebook, was proposed. Very recently, in [16], the overhead and challenges brought by the RIS network integration were discussed. It was argued that the reduced overhead offered by codebook-based RIS configuration schemes, is beneficial to the overall system performance. Nevertheless, the required control information that need to be exchanged for those schemes was not investigated. In [19] and [20], a detailed protocol for RIS-aided communication system was presented tackling the initial access problem. It was showcased that, despite the configuration control overhead, the RIS brings notable performance benefits allowing more UEs to access the network on average. However, it was assumed that the RIS control is perfect, which can be hardly true in practice.

The effect of retransmission protocols in RIS-aided systems for cases of erroneous transmissions was studied in [21], although the presented methodology assumed perfect control signals.

There has been a significant discussion regarding the comparison of RISs and conventional amplify-and-forward relays [1]. While the distinction between them can sometimes be blurred [22], one way to make a clear distinction is the use of the flow of control and data through the communication layers [23, Fig. 2]. Those considerations set the basis for the definition of the control channel options in this paper.

### B. Contributions

The main objective of this work is to develop a framework for designing and analyzing the control channel (CC) in RIS-aided communication systems. The number of actual CC designs is subject to a combinatorial explosion, due to the large number of configurable parameters in the system, such as frame size or feedback design. Clearly, we cannot address all these designs in a single work, but what we are striving for is to get a simple, yet generic, model for analyzing the impact of CCs that captures the essential design trade-offs and can be used as a framework to analyze other, more elaborate, CC designs.

We build generic CC models along two dimensions. The *first dimension* is related to how the CC interacts with the bandwidth used for data communication. An *out-of-band CC (OB-CC)* uses communication resources that are orthogonal to the ones used for data communication. More precisely, OB-CC exerts control over the propagation environment, but is not affected by this control. Contrary to this, an *in-band CC (IB-CC)* uses the same communication resources as data communication. This implies that the IB-CC decreases the number of degrees of freedom for transmission of useful data, thereby decreasing the spectral efficiency (SE) of the overall system. Furthermore, the successful transmission of the control messages toward the RIS is dependent on its phase profile. For instance, an unfavorable RIS configuration may cause blockage of the IB-CC and transmission of further control messages, impacting the overall system performance.

The *second dimension* is built along the traditional diversity-multiplexing trade-off in wireless communication systems. In a *diversity transmission*, the data rate is predefined and the sender hopes that the propagation environment is going to support that rate. If this is not the case, then, an outage occurs. To reflect this paradigm in an RIS setup, we consider a transmission setup in which the RIS sweeps through different configurations and the BS tries to select the one that is likely to support the predefined data rate. In a *multiplexing transmission*, the data rate is adapted

to the actual channel conditions; however, this incurs more signaling for channel estimation. In an RIS-aided setup, the multiplexing transmission corresponds to a case in which the RIS configuration is purposefully configured to maximize the link signal-to-noise ratio (SNR) and the data rate is chosen accordingly.

This paper analyzes the CC performance and impact in several communication setups, obtained as combinations of the aforementioned dimensions. In doing so, we have necessarily made simplifying assumptions, such as the use of a frame of a fixed length in which the communication takes place. This is especially important when analyzing a CC performance since any flexibility will affect the design of the CC. For instance, if a frame has a flexible length that is dependent on the current communication conditions, then, this flexibility can only be enabled through specific signaling over the CC, including encoding of control information and feedback<sup>1</sup>.

*Paper Outline:* In Section II, the system model is described, while Section III describes the paradigms of communication, focusing on the general description of the methods and the description of the obtained SNR, SE, and (eventually) outage generated by the method itself *without accounting for potential control error*. Section IV describes firstly how to take into account the errors in the CCs, which generate further outages/reduction of throughput performance. Then, the methods presented in the previous section are analyzed from the control perspective. In Section V, the performance of the studied communication paradigms is evaluated, while Section VI concludes the paper.

*Notation:* Lower and upper case boldface letters denote vectors and matrices, respectively; the Euclidean norm of  $\mathbf{x}$  is  $\|\mathbf{x}\|$ ; and  $\odot$  denotes the element-wise product.  $\mathcal{P}(e)$  is the probability that event  $e$  occurs;  $\mathcal{CN}(\boldsymbol{\mu}, \mathbf{R})$  is the complex Gaussian distribution with mean  $\boldsymbol{\mu}$  and covariance matrix  $\mathbf{R}$ ,  $\text{Exp}(\lambda)$  is the exponential distribution with mean value  $1/\lambda$ .  $\mathbb{E}[\cdot]$  is the expected value,  $\lfloor a \rfloor$  is the nearest lower integer of  $a$ , and  $j \triangleq \sqrt{-1}$ .

## II. SYSTEM MODEL

Let us consider the simple uplink (UL) scenario depicted in Fig. 1, which consists of a single-antenna BS, a single-antenna UE, and a fully-reflective RIS. The RIS has  $N$  elements equally spaced on a planar surface. Each RIS element is able to change the phase shift of an

<sup>1</sup>The simulation code for the paper is available at <https://github.com/lostinafro/ris-control>

incoming wave by  $\varphi_n \in [0, 2\pi]$ ,  $\forall n \in \mathcal{N}^2$ . We denote as  $\boldsymbol{\phi} = [e^{j\varphi_1}, \dots, e^{j\varphi_N}]^\top \in \mathbb{C}^N$  the vector representing a particular *configuration* of the phase shifts of the elements at a given time. A RIS controller (RISC) is in charge of loading different configurations to the RIS surface. The RISC is equipped with a look-up table containing a set of predefined configurations  $\mathcal{C}$ ,  $|\mathcal{C}| = C$ ; a copy of this look-up table is stored in the BS, so that the BS can send control signals to instruct the RISC to load a configuration already stored in  $\mathcal{C}$ . Therefore, the set  $\mathcal{C}$  is the so-called *common codebook* of configurations. Remark that the BS can also issue a command to load a configuration not present in the common codebook by sending the explicit phase-shift values for each RIS element.

To study the impact of the control signals on communication, we focus on characterizing three narrowband<sup>3</sup> wireless channels: *a)* the UE-data channel (DC), where the UE sends payload data to the BS, *b)* the UE-CC, in which the BS and the UE can share control messages to coordinate their communication, and *c)* the RIS-CC that connects the BS to the RISC so that the former can control the operation of the latter. Fig. 1 illustrates the channels further detailed below.

*a) UE-DC:* This narrowband channel operates with frequency  $f_d$  and bandwidth  $B_d$ . The UL SNR over the data channel is

$$\gamma = \frac{\rho_u}{\sigma_b^2} |\boldsymbol{\phi}^\top (\mathbf{h}_d \odot \mathbf{g}_d)|^2 = \frac{\rho_u}{\sigma_b^2} |\boldsymbol{\phi}^\top \mathbf{z}_d|^2, \quad (1)$$

where  $\mathbf{h}_d \in \mathbb{C}^N$  is the data channel from the UE to the RIS, while  $\mathbf{g}_d \in \mathbb{C}^N$  defines the one from the RIS to the BS. For simplicity of notation, we define the equivalent channel as  $\mathbf{z}_d = (\mathbf{h}_d \odot \mathbf{g}_d) \in \mathbb{C}^N$ . The UE transmit power is  $\rho_u$  and  $\sigma_b^2$  is the noise power at the BS radio frequency (RF) chain. In the remainder of the paper, we assume that the BS knows the values of  $\rho_u$  and  $\sigma_b^2$ : the transmit power is usually determined by the protocol or set by the BS itself; the noise power can be considered static for a time horizon longer than the coherence time and hence estimated previously through standard estimation techniques, *e.g.*, [24].

<sup>2</sup>For the sake of simplicity and following the standard practice in literature, we consider an ideal RIS to show the theoretical performance achievable by the system at hand. We expect that more realistic models addressing attenuation, mutual coupling, and non-linear effects would reduce the overall performance [8].

<sup>3</sup>The narrowband assumption of the channel is considered to simplify the analysis done throughout the paper in order to focus on the timing of the operations needed in the control and data channels to successfully perform a RIS-aided wireless transmission, as specified in Sects. III and IV. Nevertheless, the system aspects of the control channel can be carried over to a wideband or orthogonal frequency-division multiplexing (OFDM) case.

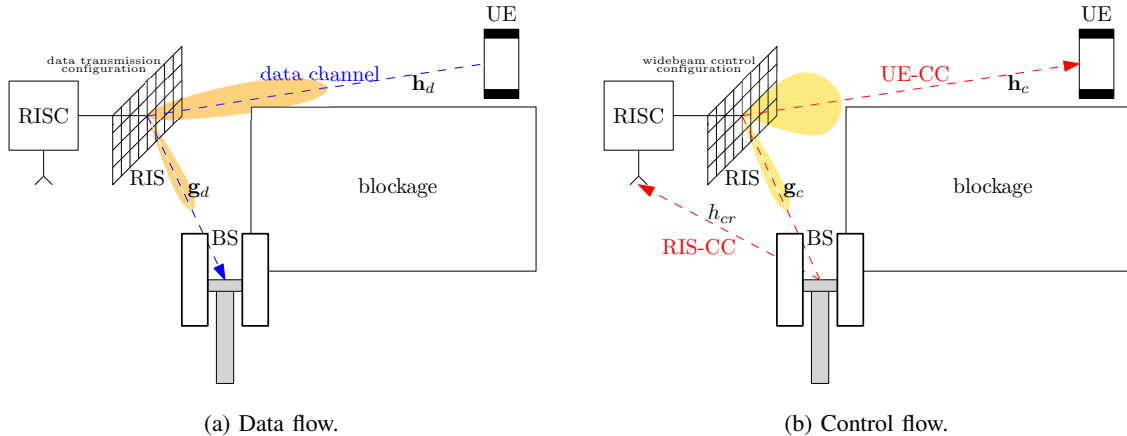


Fig. 1: Scenario of interest: RIS extends the coverage of the BS, which has a blocked link to the UE. During data transmission, the RISC loads a configuration aiming to achieve a certain communication performance; during control signaling, the RISC loads a wide beamwidth configuration to deliver low-rate control packets to the UE.

*b) UE-CC:* This narrowband channel operates on central frequency  $f_u$  and bandwidth  $B_u$  and is assumed to be a wireless IB-CC, meaning that the physical resources employed for the UE-CC overlaps the one used for the UE-DC, *i.e.*,  $f_u = f_d$ , and  $B_u \geq B_d$ . To ensure that the UE control messages reflected by the RIS reach the BS and vice-versa, we consider that the RIS makes use of a wide beamwidth configuration, termed *control (ctrl) configuration*. Wide beamwidth radiation patterns generally offer increased robustness in terms of outage probabilities when low data rates are needed [25], which makes them an ideal choice for ctrl configurations. Without loss of generality, we assume that the RISC loads the ctrl configuration anytime it is in an idle state. In other words, if the RISC has not been triggered to load other configurations, the ctrl configuration is loaded. In those cases, the UE-CC channel is described by

$$h_{cu} = \phi_{\text{ctrl}}^T (\mathbf{h}_c \odot \mathbf{g}_c) = \phi_{\text{ctrl}}^T \mathbf{z}_c, \quad (2)$$

where  $\phi_{\text{ctrl}}$  is the ctrl configuration and  $\mathbf{h}_c \in \mathbb{C}^N$  and  $\mathbf{g}_c \in \mathbb{C}^N$  are the UE-RIS and RIS-UE CCs, respectively. The equivalent end-to-end channel is  $\mathbf{z}_c = \mathbf{h}_c \odot \mathbf{g}_c \in \mathbb{C}^N$ . Herein, we do not focus on designing the ctrl configuration, whose design can be based on other works (*e.g.*, see the configuration design proposed in [15]). Instead, we assume that the above channel in (2) is Gaussian distributed as  $h_{cu} \sim \mathcal{CN}(0, \tilde{\lambda}_u)$  with  $\tilde{\lambda}_u$  being a term accounting for the (known) large-scale fading dependent on the ctrl configuration. Hence, the SNR measured at the UE is

$$\Gamma_u = \frac{\rho_b}{\sigma_u^2} |h_{cu}|^2 \sim \text{Exp} \left( \frac{1}{\lambda_u} \right), \quad (3)$$

where  $\lambda_u = \frac{\rho_b \tilde{\lambda}_u}{\sigma_u^2}$  denotes the average SNR at the UE, being  $\rho_b$  the BS transmit power and  $\sigma_u^2$  the UE's RF chain noise power.

c) *RIS-CC*: We assume that the RIS-CC is narrowband having central frequency  $f_r$ , bandwidth  $B_r$ , and channel coefficient denoted as  $h_{cr} \in \mathbb{C}$ . To obtain simple analytic results, we assume that the BS-RISC coefficient can be modeled as  $h_{cr} \sim \mathcal{CN}(0, \tilde{\lambda}_r)$  where  $\tilde{\lambda}_r$  accounts for the large-scale fading, assumed known. Therefore, the SNR measured at the RISC results

$$\Gamma_r = \frac{\rho_b}{\sigma_r^2} |h_{cr}|^2 \sim \text{Exp} \left( \frac{1}{\lambda_r} \right), \quad (4)$$

where  $\lambda_r = \frac{\rho_b \tilde{\lambda}_r}{\sigma_r^2}$  denotes the average SNR at the RISC receiver, being  $\sigma_r^2$  the noise power at its RF chain. Remark that this channel can be either: *i*) *IB-CC* meaning that the physical resources employed by the UE-DC are overlapped by the one used by the RIS-CC, *i.e.*,  $f_r = f_d$ ,  $B_r \geq B_d$ ; or *ii*) *OB-CC*, where the physical resources of the control channel are not consuming degrees of freedom from the data-transmission resources, thereby simulating a cabled connection between the decision maker and the RISC. In the case of *OB-CC*, we further assume that the RIS-CC is an error-free channel with feedback capabilities, *i.e.*,  $\lambda_r \rightarrow \infty$ . This is reasonable to assume, as, once it is decided to use *OB-CC*, the system designer has a large pool of reliable options.

### III. RIS-AIDED COMMUNICATION PARADIGMS

In this section, we first describe a structure and building blocks of a general RIS-aided communication paradigm that is applicable to a large number of potential systemic and algorithmic realizations. Then, we use the general paradigm to describe two particular transmission strategies and their respective systemic and algorithmic modules. We analyze their performance in terms of the expected SNR and SE while describing the errors eventually occurring during their operation.

#### A. General paradigm structure

Throughout the remainder of the paper, we assume that the system operates based on frames with duration,  $\tau$ , shorter than the channel coherence time, *i.e.*, the channel coefficients are assumed to be constant – or change negligibly – over the duration of the frame. The channel coherence time is considered to be estimated beforehand and hence known at the beginning of each frame. Within each frame, a RIS-aided communication paradigm can be divided into four main phases, namely “*Setup*”, “*Algorithmic*”, “*Acknowledgement*”, and “*Payload*”, described in the following. We note that there could be access algorithms in which some of these phases

may not be present; however, the mentioned four phases set a basis for a sufficiently general framework that can be used, in principle, to design other schemes where some of the steps are merged or omitted.

*Setup:* The communication procedure starts with the Setup phase; it is typically initiated by the BS and relies on control signaling to notify the RIS and the scheduled UE about the start of the new round of transmissions, *i.e.*, a frame. It is assumed that the RISC loads the ctrl configuration at the beginning of this phase. The duration of this phase is denoted with  $\tau_{\text{set}} < \tau$  and it depends on the type of available CC. Although not considered in this paper, the Setup phase can also incorporate the random access phase as an intermediate step where the scheduling and resource allocation needs of the UEs are determined.

*Algorithmic:* After the Setup is performed, the Algorithmic phase starts. In general, this phase encompasses all the processes and computations that are needed to optimize the data transmission taking place later on. This phase has a duration  $\tau_{\text{alg}} < \tau$  that depends on the choice of the employed communication paradigm. Apart from the evaluation of an appropriate RIS configuration enabling the data transmission, other objectives could be to determine the transmission parameters for the UE, and/or BS beamforming, etc. To tackle these objectives, some form of sensing of the wireless environment is required, typically enabled by the transmission of pilot sequences. The specifications of those pilots, *i.e.* their number, design, whether they are transmitted in the UL or downlink (DL), whether feedback is available, etc., are implementation- and system-defined. The computational nodes of the system (usually, the BS) use the collected pilot signals and invoke pre-defined algorithms to determine the aforementioned transmission parameters to be used in the Payload phase. The outcome of these algorithms might be affected by different types of *algorithmic errors* that might prevent the system to perform as expected, and thus should be taken into account when analyzing the overall performance.

*Acknowledgement:* The Acknowledgement phase starts once the Algorithmic phase ends; during this phase, the RIS configuration chosen needs to be communicated to the RISC, which in turn commands the RIS to load the specified phase shifts. Additionally, some further control signaling may occur between the BS and the UE as a final check before the data transmission, for example, to set the modulation and coding scheme (MCS). It is implied that the RISC loads the ctrl configuration at the beginning of this phase. Similar to the Setup phase, the Acknowledgement phase duration  $\tau_{\text{ack}} < \tau$ , depends on the type of CC used.

*Payload:* The payload phase is the last one, during which the actual data transmission takes place, which is in the UL for this work. This phase spans a duration  $\tau_{\text{pay}} < \tau$  until the end of the channel coherence frame. This phase may or may not include the feedback at the end; this aspect is not considered in this paper.

In the following subsections, we describe two state-of-the-art paradigms for RIS-aided communications employing different approaches for the Algorithmic phase. The first is the *optimization based on channel estimation (OPT-CE)*, which follows a standard multiplexing transmission: the UE's channel state information (CSI) is evaluated at the BS, which then uses this information to compute the RIS' optimal configuration and the corresponding achievable data rate. The BS sends the optimal configuration to the RISC, which loads it to the RIS surface, while the UE is instructed to transmit the data using the stipulated MCS. The second approach is the *codebook-based beam sweeping (CB-BSW)*, which was formally defined as a communication paradigm in [16], but already used in previous works (*e.g.*, [19]). This paradigm resembles the concept of diversity transmission. Here the BS does not spend time figuring out the best configuration to improve the quality of the UE-DC and does not tune the transmission rate; it instead applies a best-effort strategy, as in every diversity-oriented transmission. Specifically, the BS instructs the RISC to sweep through a set of predefined configurations – *the configuration codebook* – and hopes that at least one will satisfy a target key performance indicator (KPI) *a priori* specified for the transmission (*e.g.*, a minimum SNR to support a predefined rate). Fig. 2 shows the data exchange diagrams of the two paradigms comprised of CC messages, configuration loading, processing operations, and data transmission. Based on these, a detailed description of the two paradigms is given in the following sections. The details on the design and reliability of the messages being sent through the CCs are given in Sect. IV.

### B. Optimization based on channel estimation (OPT-CE)

For this communication paradigm, the BS needs to obtain the CSI for the UE in order to optimize the RIS configuration. The necessary measurements can be collected through the transmission of pilot sequences from the UE. During the Setup phase, the BS informs the other entities that the procedure is starting: the UE is informed through the UE-CC to prepare to send pilots. To solve the indeterminacy of the  $N$  path CE problem because of the presence of the RIS [26], the RIS is instructed to sweep through a common codebook of configurations during the Algorithmic phase called *channel estimation codebook* and denoted as  $\mathcal{C}_{\text{CE}} \subseteq \mathcal{C}$ . To change

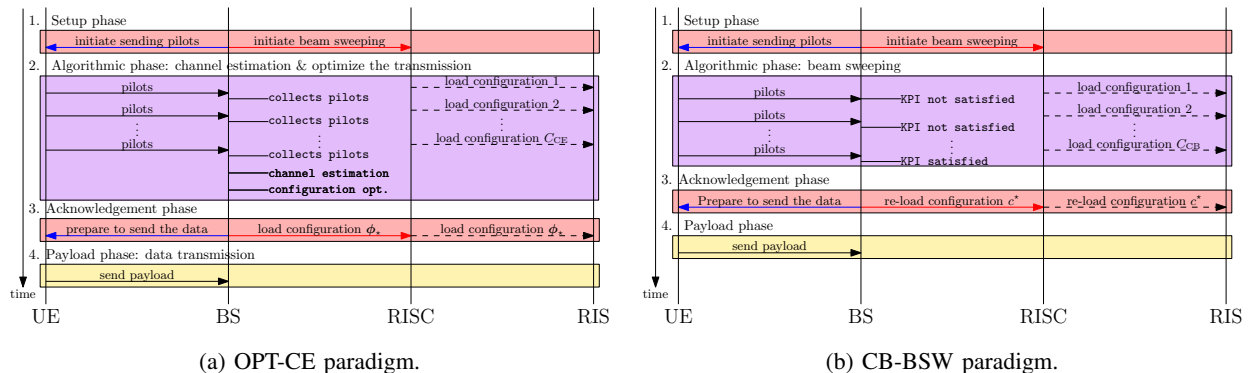


Fig. 2: Data exchange diagram of the two RIS-aided communication paradigms. Signals traveling through RIS-CC, UE-CC, and UE-DC are represented by solid red, solid blue and solid black lines, respectively. RISC to RIS commands are indicated with dashed black lines. BS operations are in monospaced font.

between the configurations in the channel estimation codebook, the BS needs to send only a single control message to the RISC since the RIS sweeps following the order stipulated by the codebook. During the Algorithmic phase, the UE sends replicas of its pilot sequence subject to different RIS configurations to let each of them experience a different propagation environment. After a sufficient number of samples is received, the BS can estimate the CSI and compute the optimal RIS's configuration. Then, the Acknowledgement phase starts, in which the BS informs the UE over the UE-CC to start sending data by using the ctrl configuration<sup>4</sup> and, subsequently, the BS informs the RISC over the RIS-CC to load the optimal configuration. Finally, the Payload phase takes place.

*Performance Analysis:* We now present the CE procedure and analyze its performance in connection to the cardinality of the employed codebook  $C_{CE} = |C_{CE}|$ . The method employed can be seen as a simplification of the method proposed in [26]. Let us start with the pilot sequence transmission and processing. We denote a single pilot sequence as  $\psi \in \mathbb{C}^p$ , spanning  $p$  symbols and having  $\|\psi\|^2 = p$ . Every time a configuration from the codebook is loaded at the RIS, the UE sends a replica of the sequence  $\psi$  towards the BS. When configuration  $c \in C_{CE}$  is

<sup>4</sup>We remark that the ctrl configuration is automatically loaded after the Algorithmic phase ends, due to the idle state of the RIS. Another approach is loading the optimal configuration evaluated in the Algorithmic phase also to send the control information toward the UE; nevertheless, the RISC needs to be informed previously by a specific control message by the BS. We do not consider this approach to keep the frame structure of the two paradigms similar and the analysis complexity at the minimum, simplifying the presentation of Sect. IV.

loaded, the following signal is received at the BS:

$$\mathbf{y}_c^\top = \sqrt{\rho_u} \boldsymbol{\phi}_c^\top \mathbf{z}_d \boldsymbol{\psi}^\top + \tilde{\mathbf{w}}_c^\top \in \mathbb{C}^{1 \times p}, \quad (5)$$

where  $\boldsymbol{\phi}_c$  denotes the phase-shift profile vector of the configuration  $c \in \mathcal{C}_{\text{CE}}$ ,  $\rho_u$  is the transmit power, and  $\tilde{\mathbf{w}}_c \sim \mathcal{CN}(0, \sigma_b^2 \mathbf{I}_p)$  is the additive white gaussian noise (AWGN). The received symbol is then correlated with the pilot sequence and normalized by  $\sqrt{\rho_u p}$ , obtaining

$$y_c = \frac{1}{\sqrt{\rho_u p}} \mathbf{y}_c^\top \boldsymbol{\psi}^* = \boldsymbol{\phi}_c^\top \mathbf{z}_d + w_c \in \mathbb{C}, \quad (6)$$

where  $w_c \sim \mathcal{CN}(0, \frac{\sigma_b^2}{p\rho_u})$  is the resulting AWGN<sup>5</sup>. The pilot transmissions and the processing in eq. (6) are repeated for all configurations,  $\forall c \in \mathcal{C}_{\text{CE}}$ . The resulting signal  $\mathbf{y} \in \mathbb{C}^{C_{\text{CE}}} = [y_1, y_2, \dots, y_{C_{\text{CE}}}]^\top$  can be written in the following form:

$$\mathbf{y} = \boldsymbol{\Theta}^\top \mathbf{z}_d + \mathbf{w}, \quad (7)$$

where  $\boldsymbol{\Theta} = [\boldsymbol{\phi}_1, \boldsymbol{\phi}_2, \dots, \boldsymbol{\phi}_{C_{\text{CE}}}] \in \mathbb{C}^{N \times C_{\text{CE}}}$  is the matrix containing all the configurations employed and  $\mathbf{w} = [w_1, \dots, w_{C_{\text{CE}}}]^\top \in \mathbb{C}^{C_{\text{CE}} \times 1}$  is the noise term. For the sake of generality, we will assume that there is no prior information about the channel distribution at the BS. Therefore, we cannot estimate separately  $\mathbf{h}_d$  and  $\mathbf{g}_d$ , but only the equivalent channel  $\mathbf{z}_d$ . It is possible to show that a necessary (but not sufficient) condition to perfectly estimate the channel coefficients is that  $C_{\text{CE}} \geq N$  [26]. Indeed, we want to have a linearly independent set of equations, which can be obtained by constructing the configuration codebook for CE to be at least rank  $N$ . As an example, we can use the discrete Fourier transform (DFT) matrix, *i.e.*,  $[\boldsymbol{\Theta}]_{n,i} = e^{-j2\pi \frac{(n-1)(c-1)}{C_{\text{CE}}}}$ ,  $n = \{1, \dots, N\}$ ,  $c \in \mathcal{C}_{\text{CE}}$ , with  $\boldsymbol{\Theta}^* \boldsymbol{\Theta}^\top = C_{\text{CE}} \mathbf{I}_N$ . Considering that the parameter vector of interest is deterministic, the least-squares estimate [28] yields

$$\hat{\mathbf{z}}_d = \frac{1}{C_{\text{CE}}} \boldsymbol{\Theta}^* \mathbf{y} = \mathbf{z}_d + \mathbf{n}, \quad (8)$$

where  $\mathbf{n} \sim \mathcal{CN}(0, \frac{\sigma_b^2}{p\rho_u C_{\text{CE}}} \mathbf{I}_N)$  and whose performance is proportional to  $1/C_{\text{CE}}$ . Based on the estimated equivalent channel, the BS can obtain the configuration  $\boldsymbol{\phi}_*$  that maximizes the instantaneous SNR of the typical UE as follows

$$\boldsymbol{\phi}_* = \max_{\boldsymbol{\phi}} \{ |\boldsymbol{\phi}^\top \hat{\mathbf{z}}_d|^2 \mid \|\boldsymbol{\phi}\|^2 = N \}, \quad (9)$$

<sup>5</sup>The consideration of dividing the pilot transmission over configurations over small blocks of  $p$  symbols basically serves three purposes: *i*) from the hardware point of view, it might be difficult to change the phase-shift profile of a RIS within the symbol time, *ii*) to reduce the impact of the noise, and *iii*) to have the possibility of separating up to  $p$  UE's data streams, if the pilots are designed to be orthogonal to each other [27].

which turns out to provide the intuitive solution of setting  $(\phi_\star)_n = e^{-j\angle(\hat{\mathbf{z}}_d)^n}$ ,  $\forall n = \{1, \dots, N\}$ . Finally, the UL estimated SNR at the BS results

$$\hat{\gamma}_{\text{CE}} = \frac{\rho_u}{\sigma_b^2} |\phi_\star^\top \hat{\mathbf{z}}_d|^2. \quad (10)$$

Based on the estimated SNR, the SE of the data communication can be adapted to be the maximum achievable, *i.e.*,

$$\eta_{\text{CE}} = \log_2(1 + \hat{\gamma}_{\text{CE}}). \quad (11)$$

*Algorithmic errors:* For the OPT-CE paradigm, a communication outage occurs in the case of an *overestimation error*, *i.e.*, if the selected SE  $\eta_{\text{CE}}$  is higher than the actual channel capacity leading to an unachievable communication rate [29]. The probability of this event is

$$p_{\text{ae}} = \mathcal{P}[\eta_{\text{CE}} = \log(1 + \hat{\gamma}_{\text{CE}}) \geq \log_2(1 + \gamma_{\text{CE}})], \quad (12)$$

where  $\gamma_{\text{CE}} = \frac{\rho_u}{\sigma_b^2} |\phi_\star^\top \mathbf{z}_d|^2$  is the actual SNR at the BS. Eq. (12) translates to the condition

$$p_{\text{ae}} = \mathcal{P}[\hat{\gamma}_{\text{CE}} \geq \gamma_{\text{CE}}] = \mathcal{P}[|\phi_\star^\top \mathbf{z}_d + \phi_\star^\top \mathbf{n}|^2 \geq |\phi_\star^\top \mathbf{z}_d|^2]. \quad (13)$$

A formal analysis of eq. (13) depends on the channel model of  $\mathbf{z}_d$ , and, hence, on making a prior assumption on the scenario at hand. To keep the analysis general, we resort to numerical methods to evaluate the impact of the OPT-CE algorithmic error.

### C. Codebook-based beam sweeping (CB-BSW)

In the Setup phase, the BS commands the start of a new frame by signaling to the RIS and the UE. During the Algorithmic phase, a *beam sweeping process* and the configuration selection are performed. The beam-sweeping process comprises the UE sending reference signals, while the BS commands the RIS to change its configuration at regular time periods accordingly to a set of common configurations, labeled as the *beam-sweeping codebook* and denoted by the symbol  $\mathcal{C}_{\text{CB}} \subseteq \mathcal{C}$ . The BS receives the reference signals that are used to measure the UE's KPI. Again, a single BS control message received by the RISC is enough to trigger the whole sweeping process. At the end of the beam-sweeping process, the BS selects a configuration satisfying the target KPI. During the Acknowledgment phase, the BS informs the UE over the UE-CC to prepare to send data by using the ctrl configuration and informs the RISC through the RIS-CC to load the selected configuration. Finally, the Payload phase takes place.

We consider that the beam-sweeping process occurring in the Algorithmic phase may make use of i) a *fixed* or ii) a *flexible* frame structure. The former is based on a fixed number of configurations in the beam-sweeping codebook: the beam-sweeping process ends after the last configuration in the codebook is loaded. The latter allows stopping the beam-sweeping earlier, as soon as a KPI value measured is above the target one. Enabling the flexible structure method requires that the BS makes the KPI measurements on-the-fly; moreover, resources on the UE-CC need to be reserved to promptly communicate to the UE to stop sending pilot sequences when the target KPI is met, modifying the organization of the overall frame. A detailed description of these differences and the impact on the CCs design are given in Sect. IV.

*Performance analysis:* In order to study the beam sweeping performance, let us assume that the target KPI is a target SNR  $\gamma_0$  measured at the BS from the average received signal strength (RSS). Therefore, in this case we have a fixed SE defined *a priori* given by

$$\eta_{\text{CB}} = \log_2(1 + \gamma_0), \quad (14)$$

and we aim to find a configuration from the codebook that supports such SE. Let us then analyze the system by starting from the pilot sequence transmission and processing. As before, every pilot sequence consists of  $p$  symbols<sup>6</sup>. Once again, we denote a single sequence as  $\boldsymbol{\psi} \in \mathbb{C}^p$  having  $\|\boldsymbol{\psi}\|^2 = p$ . After the RIS has configuration  $c \in \mathcal{C}_{\text{CB}}$  loaded, the UE sends a replica of the sequence  $\boldsymbol{\psi}$ ; the following signal is obtained at the BS:

$$\mathbf{y}_c^\top = \sqrt{\rho_u} \boldsymbol{\phi}_c^\top \mathbf{z}_d \boldsymbol{\psi}^\top + \tilde{\mathbf{w}}_c^\top \in \mathbb{C}^{1 \times p}, \quad (15)$$

which has the same formulation of eq. (5), where  $\boldsymbol{\phi}_c$  now denotes the configuration  $c \in \mathcal{C}_{\text{CB}}$ . The received signal is then correlated with the pilot symbol and normalized by  $p$ , obtaining

$$y_c = \frac{1}{p} \mathbf{y}_c^\top \boldsymbol{\psi}^* = \sqrt{\rho_u} \boldsymbol{\phi}_c^\top \mathbf{z}_d + w_c \in \mathbb{C}, \quad (16)$$

where  $w_c \sim \mathcal{CN}(0, \frac{\sigma_b^2}{p})$  is the resulted AWGN. The SNR provided by the configuration can be estimated by taking the absolute square of the sample and dividing it by the (known) noise variance as

$$\hat{\gamma}_c = \frac{|y_c|^2}{\sigma_b^2} = \underbrace{\frac{\rho_u}{\sigma_b^2} |\boldsymbol{\phi}_c^\top \mathbf{z}_d|^2}_{\gamma_c} + 2\Re \left\{ \frac{\sqrt{\rho_u}}{\sigma_b^2} \boldsymbol{\phi}_c^\top \mathbf{z}_d w_c \right\} + \frac{|w_c|^2}{\sigma_b^2}, \quad (17)$$

<sup>6</sup>The pilot sequences for OPT-CE and CB-BSW can be different and have different lengths. In practice, they should be designed and optimized for each of those approaches, which is beyond the scope of this paper. The same notation to denote the length of the pilot sequence in both paradigms is used for simplicity.

where  $|w_c|^2/\sigma_b^2 \sim \text{Exp}(p)$ . It is worth noting that the estimated SNR is affected by the exponential error generated by the noise, but also by the error of the mixed product between the signal and the noise, whose probability distribution function (pdf) depends on the pdf of  $\mathbf{z}_d$ . Based on eq. (17), we can select the best configuration  $c^* \in \mathcal{C}_{\text{CB}}$  providing the target KPI. In the following, we discuss the selection of the configuration for the two different frame structures.

*a) Fixed frame:* When the frame has a fixed structure, the sweeping procedure ends after the RIS sweeps through the whole codebook. In this case, we can measure the KPIs for all the configurations in the codebook. Then, the configuration selected for the payload phase is set to be the one achieving the highest estimated SNR among the ones satisfying the target KPI  $\gamma_0$ , that is,

$$c^* = \arg \max_{c \in \mathcal{C}_{\text{CB}}} \{\hat{\gamma}_c \mid \hat{\gamma}_c \geq \gamma_0\}. \quad (18)$$

As before, if no configuration achieves the target KPI, the communication is not feasible and we run into an outage event.

*b) Flexible frame:* When the frame has a flexible structure, the end of the sweeping process is triggered by the BS when the measured KPI reaches the target value. A simple on-the-fly selection method involves testing if the estimated SNR is greater than the target  $\gamma_0$ ; *i.e.*, after eq. (17) is obtained for configuration  $c \in \mathcal{C}_{\text{CB}}$ , we set

$$c^* = c \iff \hat{\gamma}_c \geq \gamma_0. \quad (19)$$

As soon as  $c^*$  is found, the BS communicates to both RIS and UE that the Payload phase can start, otherwise, the sweeping process continues until a configuration is selected. In case the whole codebook  $\mathcal{C}_{\text{CB}}$  is tested and no configuration satisfies condition (19), the communication is not feasible and we run into an outage event.

*Algorithmic errors:* For the CB-BSW paradigm, a communication outage occurs when no configuration in the beam sweeping codebook satisfies the target KPI, and in the case of overestimation error, which now occurs if the selected configuration provides an actual SNR lower than the target one, knowing that the estimated SNR was higher. These events are mutually exclusive, and hence their probability results in

$$\begin{aligned} p_{\text{ae}} &= \mathcal{P}[\gamma_{c^*} \leq \gamma_0 \mid \hat{\gamma}_{c^*} > \gamma_0] + \mathcal{P}[\hat{\gamma}_c \leq \gamma_0, \forall c \in \mathcal{C}_{\text{CB}}] \\ &= \mathcal{P}\left[\hat{\gamma}_{c^*} - \gamma_0 \leq \frac{|w_{c^*}|^2}{\sigma_b^2} + 2\Re\left\{\frac{\sqrt{\rho_u}}{\sigma_b^2} \phi_{c^*}^\top \mathbf{z}_d w_c\right\}\right] + \mathcal{P}[\hat{\gamma}_1 \leq \gamma_0, \dots, \hat{\gamma}_{C_{\text{CB}}} \leq \gamma_0], \end{aligned} \quad (20)$$

where  $\gamma_{c^*} = \frac{\rho_u}{\sigma_b^2} |\phi_{c^*}^\top \mathbf{z}_d|^2$  is the actual SNR, and  $\hat{\gamma}_{c^*} - \gamma_0 > 0$ . By applying Chebychev inequality, the overestimation probability term in (20) can be upper bounded by

$$\mathcal{P} \left[ \hat{\gamma}_{c^*} - \gamma_0 \leq \frac{|w_{c^*}|^2}{\sigma_b^2} + 2\Re \left\{ \frac{\sqrt{\rho_u}}{\sigma_b^2} \phi_{c^*}^\top \mathbf{z}_d w_c \right\} \right] \leq \frac{\mathbb{E} \left[ \frac{|w_{c^*}|^2}{\sigma_b^2} + 2\Re \left\{ \frac{\sqrt{\rho_u}}{\sigma_b^2} \phi_{c^*}^\top \mathbf{z}_d w_c \right\} \right]}{\hat{\gamma}_{c^*} - \gamma_0} = \frac{p^{-1}}{\hat{\gamma}_{c^*} - \gamma_0}. \quad (21)$$

From eq. (21), we infer that the higher the gap between  $\hat{\gamma}_{c^*}$  and  $\gamma_0$ , the lower the probability of error. The CB-BSW employing the fixed structure generally has a higher value of  $\hat{\gamma}_{c^*} - \gamma_0$  than the one with the flexible structure due to the use of the  $\arg \max$  operator to select the configuration  $c^*$ . Therefore, the fixed structure is generally more robust to overestimation errors. On the other hand, the evaluation of the probability that no configuration in the beam sweeping codebook satisfies the target KPI requires the knowledge of the cumulative density function (CDF) of the estimated SNR, whose analytical expression is channel model dependent and generally hard to obtain. Also in this case, we resort to numerical simulations to evaluate the impact of the CB-BSW algorithmic errors.

#### D. Trade-offs in different paradigms

The two RIS-aided communication paradigms can be seen as a generalization of the *fixed rate* and *adaptive rate* transmission approaches. Essentially, the SE of the OPT-CE is adapted to the achievable rate under the optimal configuration (see eq. (11)) obtaining the so-called multiplexing transmission, while the SE of the CB-BSW is set *a priori* according to the target KPI (see eq. (14)) obtaining a diversity transmission. Comparing eqs. (11) and (14) under the same environmental conditions, we have that

$$\eta_{\text{CB}} \leq \eta_{\text{CE}}, \quad (22)$$

where the price to pay for the higher SE of the OPT-CE paradigm is the increased overhead. Indeed, for the OPT-CE, an accurate CSI is needed for a reliable rate adaptation, which generally translates into a higher number of sequences to be transmitted by the UE compared to CB-BSW. Furthermore, after the pilot transmission, additional time and processing are required to determine the optimal configuration of the RIS. As a consequence, the SE of data transmission alone cannot be considered a fair metric of comparison, as it does not take into account the overheads generated by the communication paradigms. In the next section, we will introduce the impact of the control channel and give the main metric of the comparison.

#### IV. IMPACT OF THE CONTROL CHANNELS

In this section, we define a performance metric that simultaneously measures the performance of a RIS-aided communication scheme and the impact of the CCs over it. We then further characterize the terms regarding the overhead and the reliability of the CCs for the particular paradigms discussed in Section III.

##### A. Performance evaluation: Utility function

We start by defining a utility function measuring the communication performance by taking into account *a*) the overhead and error of the communication paradigms and *b*) the reliability of the CCs. Regarding overhead and errors of the paradigms, we consider the *goodput* metric defined as

$$R(\tau_{\text{pay}}, \eta) = (1 - p_{\text{ae}}) \frac{\tau_{\text{pay}}}{\tau} B_d \eta, \quad (23)$$

where  $1 - p_{\text{ae}}$  represents the probability that no algorithmic error occurs;  $\eta = \eta_{\text{CE}}$  in (11) or  $\eta = \eta_{\text{CB}}$  in (14) if OPT-CE or CB-BSW is employed, respectively;  $\tau_{\text{pay}}$  is the duration of the payload phase, and  $\tau$  is the overall duration of a frame. The overhead time is the time employed by the Setup, Algorithmic and Acknowledgement phases, being denoted as  $\tau_{\text{set}}$ ,  $\tau_{\text{alg}}$ , and  $\tau_{\text{ack}}$ , respectively. Accordingly, the payload time can be written as

$$\tau_{\text{pay}} = \tau - \tau_{\text{set}} - \tau_{\text{alg}} - \tau_{\text{ack}}. \quad (24)$$

While the overall frame length is fixed, the overhead time depends on the paradigm of communication, being a function of: the duration of a pilot,  $\tau_p$ , and the number of replicas transmitted; the optimization time,  $\tau_A$ ; the time to control the RIS, composed of the time employed for the transmission of the control packets to the UE (RISC),  $\tau_i^{(u)}$  ( $\tau_i^{(r)}$ ), and the time needed by the RIS to switch configuration,  $\tau_s$ .

Regarding the reliability of the CCs, we denote as  $P = P_u + P_r$  the total number of control packets needed to let a communication paradigm work, where  $P_u$  and  $P_r$  are the numbers of control packets intended for the UE and the RISC, respectively. Whenever one of such packets is erroneously decoded or lost, an event of *erroneous control* occurs. We assume that these events are independent of each other (and of the algorithmic errors), and we denote the probability of erroneous control on the packet  $i$  toward entity  $k \in \{u, r\}$  as  $p_i^{(k)}$ , with  $i \in \{1, \dots, P_k\}$  and  $k \in \{u, r\}$ . Erroneous controls may influence the overhead time and the communication

performance: the RIS phase-shift profile may change in an unpredictable way leading to a degradation of the performance, or worse, letting the data transmission fails. While losing a single control packet may be tolerable depending on its content, here, we assume that all the control packets need to be received correctly in order to let the communication be successful. In other words, no erroneous control event is allowed. Consequently, the probability of correct control results

$$p_{cc} = \prod_{k \in \{u,r\}} \prod_{i=1}^{P_k} (1 - p_i^{(k)}). \quad (25)$$

We are interested to show the average performance of the analyzed communication paradigms. According to the considerations made so far, the goodput is a discrete random variable having value given by (23) if correct control occurs, while it is 0 otherwise. Therefore, the average performance can be described by the following *utility function*:

$$U(\tau_{\text{pay}}, r) = \mathbb{E}_{k,i} [R(\tau_{\text{pay}}, \gamma)] = p_{cc}(1 - p_{ae}) \left( 1 - \frac{\tau_{\text{set}} + \tau_{\text{alg}} + \tau_{\text{ack}}}{\tau} \right) B_d \eta. \quad (26)$$

In the following subsections, we analyze the terms involved in eqs. (26) describing the difference between the transmission paradigms and particularizing the analysis for the different CCs.

### B. Overhead evaluation

Following the description given in Sect. III, we show the frame structures of the communication paradigms under study in Fig. 3, where the rows represent the time horizon of the packets travelling on the different channels (first three rows) and the configuration loading time at the RISC (last row). The time horizon is obtained assuming that all the operations span multiple numbers of transmission time intervals (TTIs), each of duration of  $T$  seconds, where  $\lceil \tau/T \rceil \in \mathbb{N}$  is the total number of TTIs in a frame. At the beginning of each TTI, if the RISC loads a new configuration, the first  $\tau_s$  seconds of data might be lost, due to the unpredictable response of the channel during this switching time. When needed, we will consider a guard period of  $\tau_s$  seconds in the overhead evaluation to avoid data disruption. Remember that the RISC loads the widebeam ctrl configuration any time it is in an idle state, *i.e.*, at the beginning of the Setup and Acknowledgement phases (see the ‘‘RISC’’ row of Fig. 3).

From Fig. 3, we can note that the overhead generated by Setup and Acknowledgement phases is *communication paradigm independent*<sup>7</sup>, while it is *CC dependent*. Indeed, all the paradigms

<sup>7</sup>The reliability of the control packets exchanged is still dependent on the communication paradigm, see Section IV-C.

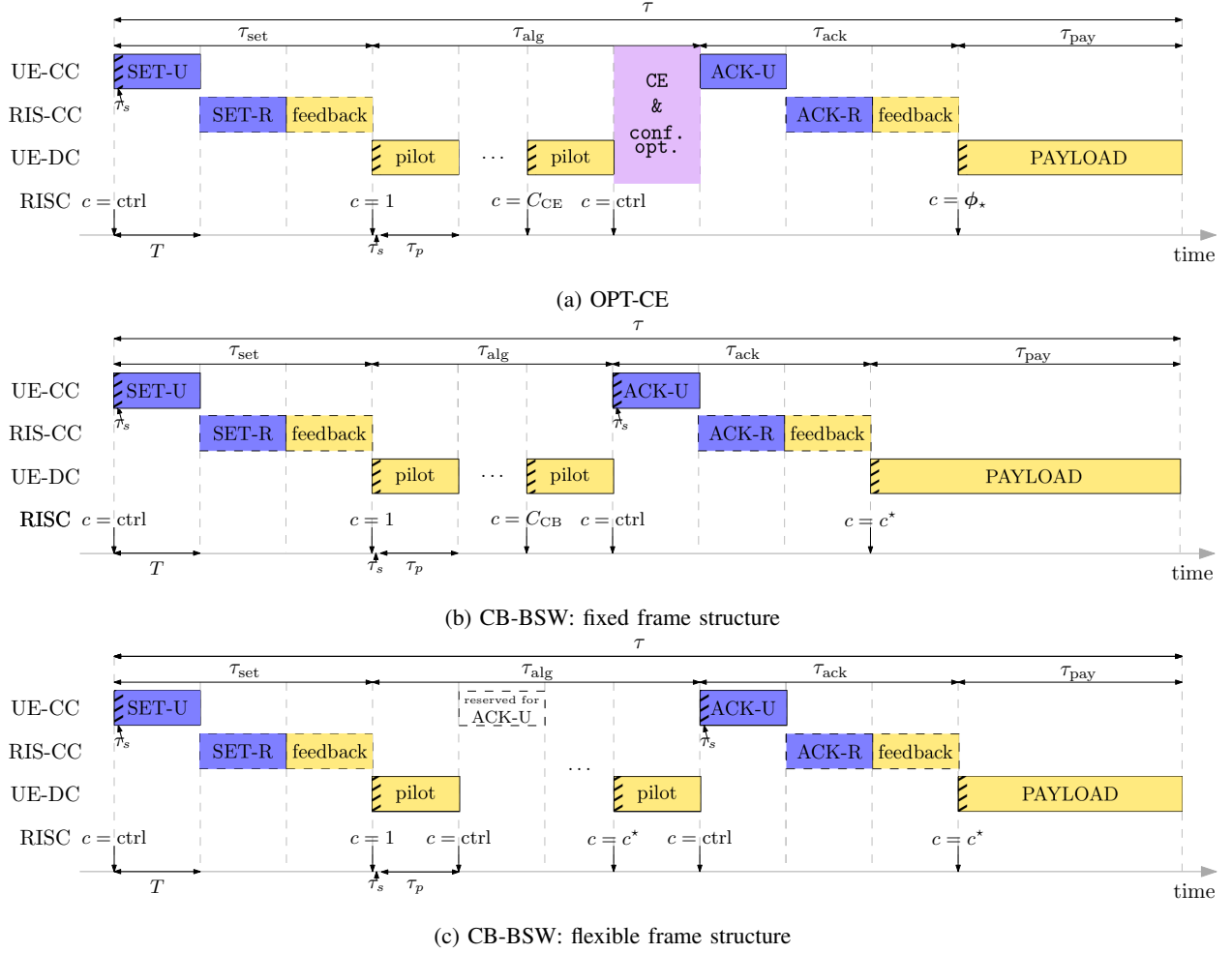


Fig. 3: Frame structure for the communication paradigms under study. Packets colored in blue and in yellow have DL and UL directions, respectively. Remark that SET-R (ACK-R) packet and its feedback are sent at the same time as the SET-U (ACK-U) but on different resources if OB-CC is present.

make use of  $P = P_u + P_r = 4$  control packets,  $P_u = 2$  control packets sent on the UE-CC and  $P_r = 2$  on RIS-CC. Nevertheless, the kind of RIS-CC employed can reduce the time employed for the communication of those packets. On the other hand, the Algorithmic phase is *CC independent* and *communication paradigm dependent* being designed to achieve the goal of the communication paradigm itself. In the following, the overhead evaluation is performed for the various cases of interest.

1) *Setup phase*: This phase starts with the SET-U control packet sent on the UE-CC, informing the UE that the OPT-CE procedure has started. If an IB-CC is employed, this is followed by the transmission of the SET-R packet to the RISC notifying the start of the procedure, and a

consequent TTI for feedback is reserved to notify back to the BS if the SET-R packet has been received. If an OB-CC is employed, no TTI needs to be reserved because the SET-R and its feedback are scheduled at the same time as the SET-U packet but on different resources. This is compliant with the assumption of error-free CC made on the definition of RIS-OB-CC in Sect. II. Accordingly, the Setup phase duration is

$$\tau_{\text{set}} = \begin{cases} T, & \text{OB-CC,} \\ 3T, & \text{IB-CC.} \end{cases} \quad (27)$$

2) *Acknowledgement phase*: The time needed to acknowledge the UE and the RISC follows the setup phase: after the optimization has run, an acknowledgment (ACK-U) packet spanning one TTI is sent to the UE notifying it to prepare to send the data; then, if a IB-CC is present, a TTI is used to send an RIS acknowledgment (ACK-R) packet containing the information of which configuration to load during the Payload phase; a further TTI is reserved for feedback. In the Setup phase, if a OB-CC is present, no TTI needs to be reserved because the ACK-R and its feedback are scheduled at the same time as the SET-U packet but on different resources. Remark that the  $\tau_s$  guard period must be considered by the UE when transmitting the data, to avoid data being disrupted during the load of the configuration employed in the Payload. For simplicity of evaluation, we insert the guard period in the overall Acknowledgement phase duration, resulting in

$$\tau_{\text{ack}} = \tau_{\text{set}} + \tau_s \quad (28)$$

3) *Algorithmic phase*: This phase comprises the process of sending pilot sequences and the consequent evaluation of the configuration for the transmission. Regardless of the paradigm, each pilot sequence spans an entire TTI, but the switching time of the configuration must be taken into account as a guard period. Therefore, the actual time occupied by a pilot sequence is  $\tau_p \leq T - \tau_s$  and the number of samples  $p$  of every pilot sequence results

$$p = \left\lfloor \frac{T - \tau_s}{T_n} \right\rfloor, \quad (29)$$

where  $T_n$  is the symbol period in seconds. Assuming that the TTI and the symbol period are fixed, the UE is able to compute the pilot length if it is informed about the guard period. On the other hand, the overall duration of the Algorithmic phase depends on the paradigm employed.

a) *OPT-CE*: In this case, the Algorithmic phase starts with  $C_{\text{CE}}$  TTIs; at the beginning of each of these TTIs, the RISC loads a different configuration, while the UE transmits replicas of the pilot sequence. After all the sequences are received, the CE process at the BS starts, followed by the configuration optimization. The time needed to perform the CE and optimization processes depends on the algorithm, as well as the available hardware. To consider a generic case, we denote this time as  $\tau_A = AT$ .

b) *CB-BSW fixed frame structure*: Similarly to the previous case, the Algorithmic phase starts with  $C_{\text{CB}}$  TTIs, at the beginning of which the RISC loads a different configuration, and the UE transmits replicas of the pilot sequence. After all the sequences are received, the BS selects the configuration as described in Sect. III-C. The time needed to select the configuration is considered negligible, and hence the Acknowledgement phase may start in the TTI after the last pilot sequence is sent.

c) *CB-BSW flexible frame structure*: In this case, the number of TTIs used for the beam sweeping process is not known *a priori* and it depends on the measured SNR. However, to allow the system to react in case the desired threshold is reached, a TTI is reserved for the transmission of the ACK-U after each TTI used for pilot transmission. Hence, the number of TTIs needed is  $2c^* - 1$ , where  $0 < c^* \leq C_{\text{CB}}$  is a random variable.

According to the previous discussion, the Algorithmic phase duration is

$$\tau_{\text{alg}} = \begin{cases} (C_{\text{CE}} + A)T, & \text{OPT-CE,} \\ C_{\text{CB}}T, & \text{CB-BSW fixed frame structure,} \\ (2c^* - 1)T, & \text{CB-BSW flexible frame structure.} \end{cases} \quad (30)$$

### C. Reliability evaluation

In this section, we evaluate the reliability of the control packets. The content of each control packet depends on the kind of control packet considered and on the communication paradigms employed, as we will describe throughout the section. Without loss of generality, we assume that the  $i$ -th control packet toward entity  $k$  comprises a total of  $b_i^{(k)}$  informative bits. Accordingly, we can express the probability of error of a single packet by means of an outage event, obtaining

$$p_i^{(k)} = \Pr \left\{ \log(1 + \Gamma_k) \leq \frac{b_i^{(k)}}{\tau_i^{(k)} B_c} \right\}, \quad k \in \{u, r\}, \quad i = \{1, 2\} \quad (31)$$

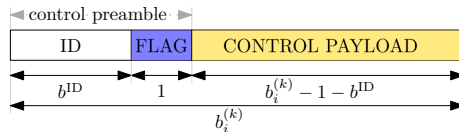


Fig. 4: General control packet structure comprising a preamble and a payload part.

where  $\tau_i^{(k)}$  is the time employed by the transmission of the  $i$ -th control packet intended for entity  $k \in \{u, r\}$ , and  $B_c$  is the CC transmission bandwidth. According to the assumption on the channel distribution, eq. (31) can be rewritten as

$$p_i^{(k)} = 1 - \exp \left\{ -\frac{1}{\lambda_k} \left( 2^{b_i^{(k)}/\tau_i^{(k)}/B_c} - 1 \right) \right\}. \quad (32)$$

Plugging eq. (32) into (25), the correct control probability for the paradigms under tests results

$$p_{cc} = \exp \left\{ \frac{1}{\lambda_u} \left( 2 - \sum_{i=1}^2 2^{b_i^{(u)}/\tau_i^{(u)}/B_c} \right) \right\} \exp \left\{ \frac{1}{\lambda_r} \left( 2 - \sum_{i=1}^2 2^{b_i^{(r)}/\tau_i^{(r)}/B_c} \right) \right\}. \quad (33)$$

In the following, we evaluate the time occupied by the transmission of the control packets  $\tau_i^{(k)}$  and the number of informative bits contained in the control packets  $b_i^{(k)}$ .

1) *Useful time for control packets:* Following the data frame, each control packet spans an entire TTI. However, the *useful time*  $\tau_i^{(k)}$ , *i.e.*, the time in which informative bits can be sent without risk to be disrupted, depends on the RIS switching time. As already discussed in Sect. IV-B, a guard period of  $\tau_s$  seconds must be considered if the RISC loads a new configuration in that TTI. Following the frame structure of Fig. 3, the SET-R and ACK-R packets can use the whole TTI, while the SET-U packets need the guard period. Note that the ACK-U control packet does not employ the guard period under the OPT-CE, as long as the time employed by the optimization process is at least a TTI, *i.e.*,  $A \geq 1$ . For the CB-BSW paradigm, the guard period is needed. As a consequence, the useful time of the packets intended for the UE results

$$\tau_1^{(u)} = T - \tau_s, \quad \tau_2^{(u)} = \begin{cases} T - \tau_s, & \text{CB-BSW,} \\ T, & \text{OPT-CE,} \end{cases} \quad (34)$$

while the useful time of the packets intended for the RISC results

$$\tau_1^{(r)} = \tau_2^{(r)} = T. \quad (35)$$

2) *Control packet content*: In this part, we evaluate the minimum number of informative bits  $b_i^{(k)}$  of each control packet. Without loss of generality, we can assume a common structure for all the control packets, comprising a control preamble and control payload parts as depicted in Fig. 4. The preamble comprises  $b^{\text{ID}}$  bits representing the *unique identifier (ID)* of the destination entity in the network, and a single bit flag specifying if the packet is a SET or an ACK one. From the preamble, the UE (RISC) can understand if the control packet is meant to be decoded and how to interpret the control payload. Accordingly, the remaining number of bits,  $b_i^{(k)} - 1 - b^{\text{ID}}$ , depends on the control payload, which, in turn, depends on the kind of control packet considered and on the communication paradigms employed.

a) *OPT-CE*: To initialize the overall procedure at the UE, the payload of the SET-U packet must contain the length of the frame  $\tau$ , the cardinality of the set  $C_{\text{CE}}$ , and the guard time  $\tau_s$ . To simplify the data transmission, the frame duration can be notified through an (unsigned) integer of  $b^{\text{frame}}$  containing the number of total TTIs  $\lceil \tau/T \rceil$  set for the frame. In the same manner, we can translate the guard time into an unsigned integer representing the number of guard symbols  $\lceil \tau_s/T_n \rceil$  so as to send  $b^{\text{guard}}$  bits. Finally, another integer of  $b^{\text{conf}}$  bits can be used to represent the cardinality  $C_{\text{CE}}$  and to notify it to the UE. Remark that the minimum  $b^{\text{conf}} = \lceil \log_2(C) \rceil$ , where  $C$  is the total number of configurations stored in the common codebook. Similarly, the payload of the SET-R packets needs to contain the information of the length of the frame  $\tau$ , and the *set* of configuration  $C_{\text{CE}}$  to switch through. Also, in this case, encoding the data as integers may reduce the number of informative bits to transmit. For the frame length, the same  $b^{\text{frame}}$  bits of the SET-U packet are used. To encode the information of the set to be employed,  $b^{\text{conf}}$  bits are used to identify a single configuration in the common codebook, and thus  $C_{\text{CE}}b^{\text{conf}}$  needs to be transmitted to the RISC, one per wanted configuration. Regarding the Acknowledgement phase, we can assume that the payload of the ACK-U contains only the chosen SE of the communication  $r_{\text{CE}}$ . This can be encoded in similar manner the MCS is encoded for the 5G standard [30]: a table of predefined values indexed by  $b^{\text{SE}}$  bits. On the other hand, the payload of the ACK-R must contain the optimal phase-shift profile  $\phi_*$ , that is, a value of the phase-shift for each element. Without loss of generality, we can denote as  $b^{\text{quant}}$  the number of bits used to control each element, *i.e.*, the level of quantization of the RIS [4]. Hence, the overall number of informative bits is the number of elements to control times the level of quantization, *i.e.*,

$Nb^{\text{quant}}$ . To summarize, the packets length results

$$b_i^{(k)} = b^{\text{ID}} + 1 + \begin{cases} b^{\text{frame}} + b^{\text{guard}} + b^{\text{conf}}, & k = u, i = 1, \text{ (SET-U)}, \\ b^{\text{frame}} + C_{\text{CE}}b^{\text{conf}}, & k = r, i = 1, \text{ (SET-R)}, \\ b^{\text{SE}}, & k = u, i = 2, \text{ (ACK-U)}, \\ Nb^{\text{quant}}, & k = r, i = 2, \text{ (ACK-R)}. \end{cases} \quad (36)$$

b) *CB-BSW*: The payload of the Setup packets follows the same scheme used for the OPT-CE paradigm. The SET-U packet contains the length of the frame  $\tau$ , the cardinality of the set  $C_{\text{CB}}$ , and the guard time  $\tau_s$  translated to (unsigned) integer of  $b^{\text{frame}}$ ,  $b^{\text{guard}}$  and  $b^{\text{conf}}$  bits, respectively. The payload of the SET-R packets contains the information of the length of the frame  $\tau$ , and the *set* of configuration  $C_{\text{CB}}$  to switch through, encoded in (unsigned) integers of  $b^{\text{frame}}$  and  $C_{\text{CB}}b^{\text{conf}}$  bits, respectively. Instead, the Acknowledgement contains different information. In particular, the payload of the ACK-U is empty, according to the fixed rate transmission used by this paradigm. The payload of the ACK-R contains the configuration  $c^*$  chosen, encoded by the same  $b^{\text{conf}}$  bits representing an index in the common codebook. To summarize, the packets length results

$$b_i^{(k)} = b^{\text{ID}} + 1 + \begin{cases} b^{\text{frame}} + b^{\text{guard}} + b^{\text{conf}}, & k = u, i = 1, \text{ (SET-U)}, \\ b^{\text{frame}} + C_{\text{CB}}b^{\text{conf}}, & k = r, i = 1, \text{ (SET-R)}, \\ 0, & k = u, i = 2, \text{ (ACK-U)}, \\ b^{\text{conf}}, & k = r, i = 2, \text{ (ACK-R)}. \end{cases} \quad (37)$$

## V. NUMERICAL RESULTS

In this section, we show the performance evaluation of the communication paradigms under study. The parameters set for the simulations are given in Table I<sup>8</sup>, if not otherwise specified. The scenario is tested through Monte Carlo simulations. With respect to the scenario described in Sect. II, we consider that the BS and RIS positions  $\mathbf{x}_b$  and  $\mathbf{x}_r = (0, 0, 0)^\top$  are kept fixed, while the UE position,  $\mathbf{x}_u$ , changes at every simulation according to a uniform distribution having limits  $(-D/2, 0, 0)^\top$  and  $(D/2, D, -D)^\top$ . In this section, when referring to average performance, we implicitly assume averaging over different UE positions and noise realizations. The DC channel coefficients are evaluated considering the line-of-sight (LoS) component of  $\mathbf{h}_d$  and  $\mathbf{g}_d$  following

<sup>8</sup>In the Table,  $\nu$  is the speed of light

TABLE I: Simulation parameters.

Scenario			Communication		
Scenario side	$D$	20 m	DC frequency	$f_d$	3 GHz
BS position	$\mathbf{x}_b$	$(25, 5, 5)^\top$ m	Bandwidth of DC	$B_d$	180 kHz
RIS element spacing	$d$	$\nu/f_d/2$	UE transmit power	$\rho_u, \rho_b$	24
Number of RIS elements	$N$	100	UE/RIS noise power	$\sigma_u^2, \sigma_r^2$	-94 dBm
Paradigms			Control packet content		
Codebooks cardinality	$C_{CE}, C_{CB}^{\text{fix}}, C_{CB}^{\text{fle}}$	$N, \lceil N/3 \rceil, N$	ID bits	$b^{\text{ID}}$	8
Overall frame duration	$\tau$	[10, 200] ms	TTIs bits	$b^{\text{frame}}$	16
TTI duration	$T$	0.5 ms	Guard period bits	$b^{\text{guard}}$	16
Guard period	$\tau_s$	50 $\mu$ s	Configuration selection bits	$b^{\text{conf}}$	8
Pilot sequence length	$p$	1	SE table bits	$b^{\text{SE}}$	6
CE duration in TTIs	$A$	5	RIS quantization level bits	$b^{\text{quant}}$	2

the model of [31, Sect. II]. Note that the RIS-OB-CC uses a different operating frequency and bandwidth w.r.t. the DC ones, while, for the IB-CC, we have  $f_r = f_d$  and  $B_r = 5B_d$ . In any case, the UE-CC has operating frequency  $f_u = f_d$  and bandwidth  $B_u = 5B_d$ . The overall frame duration  $\tau$  set reflects the coherence time of the channel: a low  $\tau$  represents a high mobility environment with low coherence time, and vice versa. The TTI duration is set according to the half of the subframe duration in the OFDM 5G NR standard [30]. For the OPT-CE paradigm, the channel estimation codebook  $\mathcal{C}_{CE}$  is designed from the DFT, as described in Sect. III-B. For the sake of simplicity, the same configurations are used in the beam sweeping codebook  $\mathcal{C}_{CB}$ . In particular, the codebook used by the CB-BSW with flexible frame structure is  $\mathcal{C}_{CB}^{\text{fle}} = \mathcal{C}_{CE}$ , while the one used by the CB-BSW with fixed frame structure uses one every three configurations, to take advantage of the possible lower overhead. In the following, we divide the results into two parts: the evaluation of the paradigms performance under error-free CCs, and the investigation of the impact of CCs reliability.

#### A. Paradigms performance (error-free CCs)

Fig. 5 shows the CDF of the actual and estimated SNR to give some insight on the impact of the possible algorithm errors. From the figure, it can be inferred that the impact of the noise on the SNR estimation is generally negligible for the OPT-CE paradigm. This finding is justified by the fact that the power of the noise influencing the measurement is proportional to

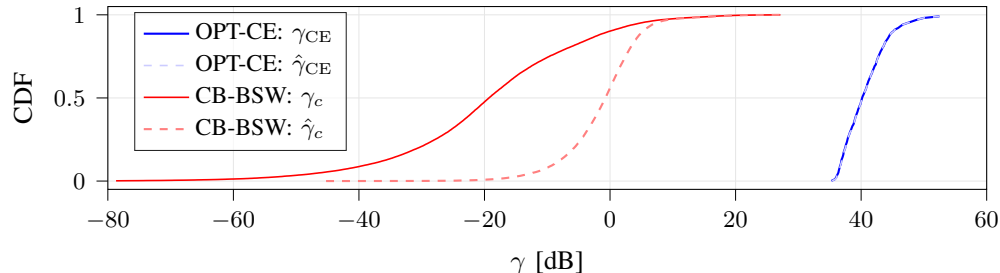


Fig. 5: CDF of the actual and estimated SNR for the communication paradigms under study.

$1/C_{CE}$ , where  $C_{CE} \geq N$  as described in Section III-B. On the other hand, when employing the CB-BSW paradigm, the measurement of the SNR is done separately per each configuration employed, and the resulting noise has a higher impact on the estimation. Moreover, we can also observe that the SNR of the CB-BSW extends to very low values, while the minimum target KPI needs to be set to provide a non-negligible and supportable SE (at least higher than -13 dB to have the minimum SE of the 5G NR standard of 0.0586 [32, Table 5.1.3.1-3]). Therefore, whatever reasonable target KPI is chosen will result in a relatively high outage probability. To summarize, the OPT-CE paradigm is inherently more robust to algorithmic errors than the CB-BSW paradigm.

To provide a fair comparison between the paradigms, we evaluate the optimal target SNR  $\gamma_0$  used as relevant KPI for the CB-BSW paradigm. Fig. 6 shows the average goodput  $R$  achieved as a function of the target SNR, under different kinds of CC and for different values of  $\tau$ . We note that the optimal  $\gamma_0$  depends on the frame structure chosen while it does not depend on the kind of CC, the latter influencing slightly the achievable goodput under the same target SNR. Moreover, the duration  $\tau$  influences negligibly the optimal  $\gamma_0$  in the flexible structure, being approx. 13.8 dB for  $\tau = 30$  ms and approx. 12.4 dB for  $\tau = 90$  ms for the flexible frame structure, while approx. 10.9 dB for any value of  $\tau$  for the fixed frame structure. We remark that the selection of the target KPI is also scenario dependent, and hence this procedure should be performed during the deployment of the RIS.

Using the optimal target SNR, we now compare the performance of the communication paradigms. Fig. 7a shows the average goodput as a function of the overall frame duration. Again, the impact of the kind of CC on the average goodput is negligible. The main advantage of the CB-BSW approach is the possibility of providing a non-null transmission rate even in

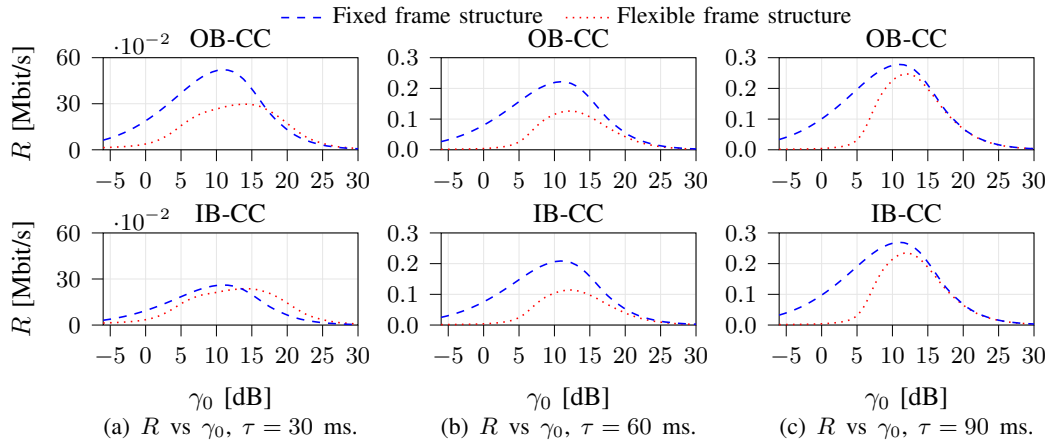


Fig. 6: Analysis of the target SNR for the CB-BSW paradigm. Note the different scale in Fig. 6a.

presence of a lower coherence block ( $< 60$  ms), while the OPT-CE needs a longer time horizon to obtain the CSI and perform the Payload phase ( $\geq 60$  ms). On the other hand, as long as the time horizon is sufficiently long ( $\tau \geq 75$  ms), the OPT-CE paradigm outperforms the CB-BSW ones. In Fig. 7b, we show the CDF of the goodput for  $\tau = 60$  ms. For this frame duration, the kind of CC influences the performance of the OPT-CE paradigm, while its impact is less predominant on the CB-BSW performance. As expected, the IB-CC provides worse performance due to its increased overhead. Nevertheless, remark that for the CB-BSW approximately half of the transmissions has null goodput because of algorithmic errors, while the OPT-CE provide a non-null goodput for all values, corroborating the results of Fig. 5.

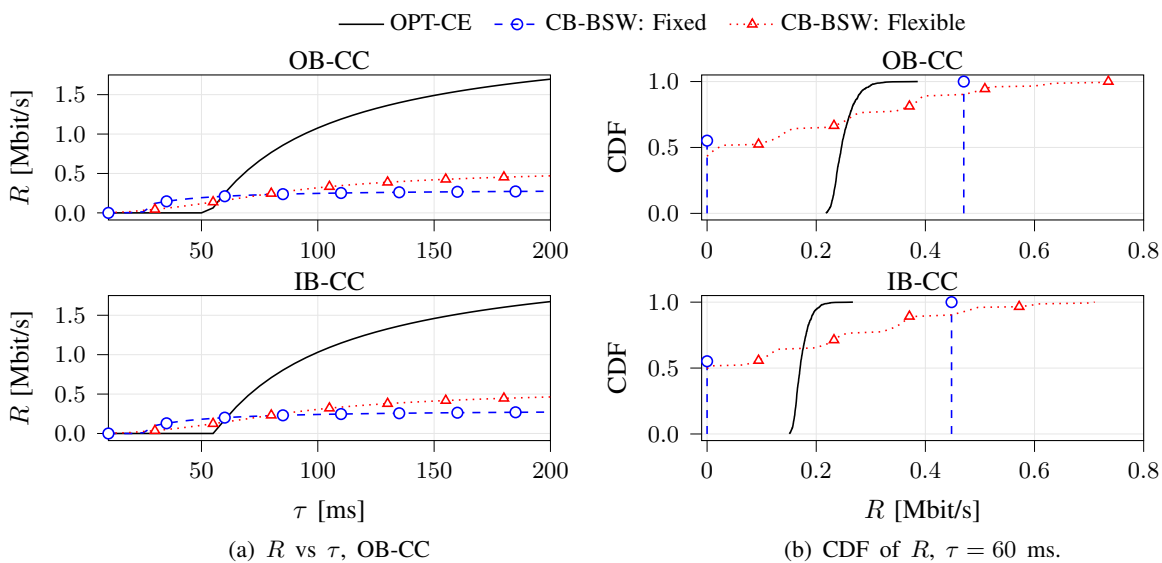


Fig. 7: Analysis of the goodput performance.

### B. Impact of the CCs reliability

Fig. 8 shows the average utility (26) as a function of the erroneous control probability  $1 - p_{cc}$ , for  $\tau = 60$  ms and for both kinds of CC. The results of the transmission paradigms are in line with the one presented in Fig. 7. The CC reliability influences significantly the performance when  $1 - p_{cc} \leq 0.05$ , *i.e.*,  $p_{cc} \leq 0.95$ . To consider a conservative case, we set a target reliability

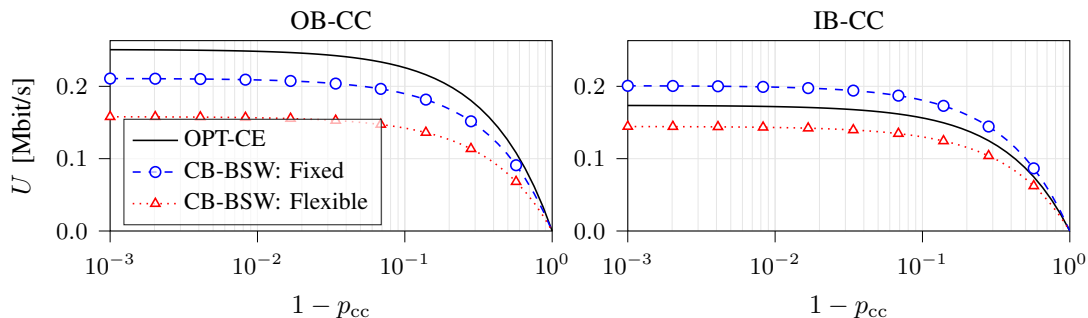


Fig. 8: Analysis of the utility function vs. erroneous control probability.

to be  $\bar{p}_{cc} = 0.99$ , and we study the minimum average SNRs  $\lambda_u$  and  $\lambda_r$  providing such reliability following the control packet content given in Table I. Fig. 9a shows the achieved  $p_{cc}$  for the OB-CC as a function of  $\lambda_u$  only, according to the assumption of error-free RIS-CC in the OB-CC case. With this kind of CC, the probabilities of correct control achieved by OPT-CE and CB-BSW have negligible differences, and a  $\bar{\lambda}_u = 10.5$  dB is enough to provide the target correct control probability in both cases. Fig. 9b shows the  $p_{cc}$  as a heatmap function of  $\lambda_r$  and  $\lambda_u$  for the IB-CC case. Note that only the region of  $\lambda_u$  and  $\lambda_r$  providing at least the target  $\bar{p}_{cc}$  is colored, while the white part of the heatmap represents the SNRs values not satisfying the target reliability. The minimum value of  $\lambda_r$  and  $\lambda_u$  needed are also given in the figure. It is worth noting that the OPT-CE needs higher SNRs than CB-BSW due to the higher information content of the control packet of the former. Finally, we remark that the performance provided by the CCs should be accounted for *simultaneously* to achieve the desired control reliability.

## VI. CONCLUSIONS

In this paper, we proposed a general framework of four phases – Setup, Algorithmic, Acknowledgement, Payload – to evaluate RIS-aided communication performance, addressing the impact of control and signaling procedures in a generic scenario. Employing this framework, we detailed the data exchange and the frame structure diagram for two different communication paradigms employed in RIS-aided communications, namely OPT-CE and CB-BSW. We analyzed

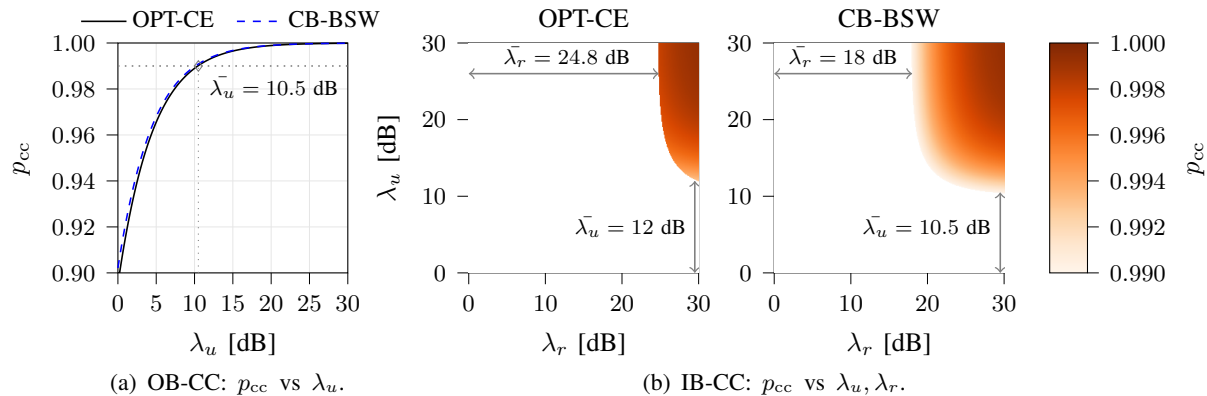


Fig. 9: Impact of the CC SNR to the reliability.

the performance considering a utility function that takes into account the overhead generated by the various phases of the paradigms, the possible errors coming from the Algorithmic phase, and the impact of losing control packets needed for signalling purposes. Moreover, we particularized the performance evaluation for two kinds of CCs connecting the decision maker and the RISC – IB-CC and OB-CC –, showcasing the minimum performance needed to obtain the desired target control reliability. While some oversimplification has necessarily been introduced, we believe that the proposed framework can be used to include the control operations into the communication performance evaluation for various scenarios of interest. For example, the framework can be applied to multi-user wideband/OFDM communications by accounting for the subcarrier allocation of the different control and payload messages. Differently from the cases studied in this paper, the Algorithmic phase should also consider the resource allocation process, whose output should be signaled to the UEs through a specific design of the Acknowledgement phase. Other potential control and algorithmic designs can be addressed by using the proposed framework, taking care of omitting, merging, or repeating some of the general phases to meet the design requirements.

## REFERENCES

- [1] C. Huang *et al.*, “Reconfigurable intelligent surfaces for energy efficiency in wireless communication,” *IEEE Trans. Wireless Commun.*, vol. 18, no. 8, pp. 4157–4170, Aug. 2019.
- [2] Q. Wu *et al.*, “Intelligent reflecting surface aided wireless communications: A tutorial,” *IEEE Trans. Commun.*, vol. 69, no. 5, pp. 3313–3351, May 2021.
- [3] E. Calvanese Strinati *et al.*, “Reconfigurable, intelligent, and sustainable wireless environments for 6G smart connectivity,” *IEEE Commun. Mag.*, vol. 59, no. 10, pp. 99–105, Oct. 2021.

- [4] G. C. Alexandropoulos *et al.*, “RIS-enabled smart wireless environments: Deployment scenarios, network architecture, bandwidth and area of influence,” *arXiv preprint arXiv:2303.08505*, 2023.
- [5] J. Chen *et al.*, “Intelligent reflecting surface: A programmable wireless environment for physical layer security,” *IEEE Access*, vol. 7, pp. 82 599–82 612, Jul. 2019.
- [6] N. Awarkeh *et al.*, “Electro-magnetic field (EMF) aware beamforming assisted by reconfigurable intelligent surfaces,” in *Proc. IEEE SPAWC*, Lucca, Italy, Sep. 2021.
- [7] M. Di Renzo *et al.*, “Communication models for reconfigurable intelligent surfaces: From surface electromagnetics to wireless networks optimization,” *Proc. IEEE*, vol. 10, no. 9, pp. 1164–1209, Sep. 2022.
- [8] M. Jian *et al.*, “Reconfigurable intelligent surfaces for wireless communications: Overview of hardware designs, channel models, and estimation techniques,” *Intell. Converged Netw.*, vol. 3, no. 1, pp. 1–32, Mar. 2022.
- [9] A. L. Swindlehurst *et al.*, “Channel estimation with reconfigurable intelligent surfaces– A general framework,” *Proc. IEEE*, vol. 10, no. 9, pp. 1312–1338, Sep. 2022.
- [10] H. Zhang *et al.*, “Channel estimation with hybrid reconfigurable intelligent metasurfaces,” *IEEE Trans. Commun.*, early access, 2023.
- [11] V. Popov *et al.*, “Experimental demonstration of a mmwave passive access point extender based on a binary reconfigurable intelligent surface,” *Frontiers Commun. Netw.*, vol. 2, p. 733891, Oct. 2021.
- [12] C. Singh *et al.*, “Fast beam training for RIS-assisted uplink communication,” *arXiv preprint arXiv:2107.14138*, 2021.
- [13] B. Zheng and R. Zhang, “Intelligent reflecting surface-enhanced ofdm: Channel estimation and reflection optimization,” *IEEE Wireless Commun.*, vol. 9, pp. 518–522, 2020.
- [14] V. Jamali *et al.*, “Low-to-zero-overhead IRS reconfiguration: Decoupling illumination and channel estimation,” *IEEE Commun. Lett.*, vol. 16, no. 4, pp. 932–936, Apr. 2022.
- [15] G. C. Alexandropoulos *et al.*, “Near-field hierarchical beam management for RIS-enabled millimeter wave multi-antenna systems,” in *Proc. IEEE SAM*, Trondheim, Norway, 2022, pp. 460–464.
- [16] J. An *et al.*, “Codebook-based solutions for reconfigurable intelligent surfaces and their open challenges,” *arXiv preprint arXiv:2211.05976*, 2022.
- [17] M. Rahal *et al.*, “Performance of RIS-aided nearfield localization under beams approximation from real hardware characterization,” *arXiv preprint arXiv:2303.15176*, 2023.
- [18] J. Wang *et al.*, “Hierarchical codebook-based beam training for RIS-assisted mmwave communication systems,” *IEEE Trans. Commun.*, early access, 2023.
- [19] V. Croisfelt *et al.*, “A random access protocol for RIS-aided wireless communications,” in *Proc. IEEE SPAWC*, 2022.
- [20] V. Croisfelt *et al.*, “Random access protocol with channel oracle enabled by a reconfigurable intelligent surface,” *arXiv preprint arXiv:2210.04230*, 2022.
- [21] S. Hao and H. Zhang, “Performance analysis of PHY layer for ris-assisted wireless communication systems with retransmission protocols,” *J. Comp. Inf. Sciences*, vol. 34, no. 8, Part A, pp. 5388–5404, 2022.
- [22] R. Long *et al.*, “Active reconfigurable intelligent surface-aided wireless communications,” *IEEE Trans. Wireless Commun.*, vol. 20, no. 8, pp. 4962–4975, Aug. 2021.
- [23] E. Björnson *et al.*, “Reconfigurable intelligent surfaces: A signal processing perspective with wireless applications,” *IEEE Signal Process. Mag.*, vol. 39, no. 2, pp. 135–158, 2022.
- [24] T. Yucek and H. Arslan, “MMSE noise power and SNR estimation for OFDM systems,” in *Proc. IEEE Sarnoff Symposium*, 2006, pp. 1–4.
- [25] M. He *et al.*, “RIS-assisted broad coverage for mmwave massive MIMO system,” in *Proc. IEEE ICC*, 2021.

- [26] Z. Wang *et al.*, “Channel estimation for intelligent reflecting surface assisted multiuser communications: Framework, algorithms, and analysis,” *IEEE Trans. Wireless Commun.*, vol. 19, no. 10, pp. 6607–6620, 2020.
- [27] E. Björnson *et al.*, “Massive MIMO networks: Spectral, energy, and hardware efficiency,” *Foundations Trends Signal Process.*, vol. 11, no. 3-4, pp. 154–655, 2017.
- [28] S. M. Kay, *Fundamentals of Statistical Signal Processing: Estimation Theory*. Prentice Hall, 1997.
- [29] C. Shannon, “Communication in the presence of noise,” *Proceedings of the IRE*, vol. 37, no. 1, pp. 10–21, 1949.
- [30] 3GPP, “Study on New Radio (NR) access technology,” 3rd Generation Partnership Project (3GPP), Technical Report (TR) 21.915, 10 2019, version 15.0.0.
- [31] A. Albanese *et al.*, “MARISA: A self-configuring metasurfaces absorption and reflection solution towards 6G,” in *Proc. IEEE INFOCOM*. IEEE, 2022, pp. 250–259.
- [32] 3GPP, “NR; Physical layer procedures for data,” 3rd Generation Partnership Project (3GPP), Technical specification (TS) 38.214, 10 2022, version 15.0.0.